

Synthesis and characterization of a fluorinated anionic aluminophosphate framework UT-6, and its high-temperature dehydrofluorination to $\text{AlPO}_4\text{-CHA}$

Scott Oliver,^a Alex Kuperman,^b Alan Lough^a and Geoffrey A. Ozin^{*a}

^aMaterials Chemistry Research Group, Lash Miller Chemical Laboratories, University of Toronto, 80 St. George Street, Toronto, Ontario, M5S 3H6, Canada

^bCatalysis Lab, The Dow Chemical Company, Midland, MI 48674, USA

The structure of an anionic aluminophosphate molecular sieve UT-6 has been determined by single-crystal X-ray diffraction and ^{19}F MAS NMR, ^{31}P CP MAS NMR and ^{27}Al MQ MAS spectroscopy. Large crystals were grown in a non-aqueous synthesis system when hydrogen fluoride was used in trace amounts. The title compound, $[\text{Al}_3\text{P}_3\text{O}_{12}\text{F}]^- [\text{C}_5\text{H}_5\text{NH}]^+ \cdot 0.15\text{H}_2\text{O}$, crystallizes in the triclinic space group $P\bar{1}$ (no. 2), with $Z=2$, $a=9.118(1)$, $b=9.161(1)$, $c=9.335(1)$ Å, $\alpha=85.98(1)$, $\beta=77.45(1)$, $\gamma=89.01(1)^\circ$, $V=759.25(14)$ Å³, $R_1=0.0280$ and $wR_2=0.0830$. UT-6 is a small pore material that has a three-dimensional network of channels running through the structure. The structure is closely related to that of chabazite. In addition to alternating tetrahedral phosphorus and aluminium atoms connected by bridging oxygens, there are also isolated pairs of octahedral aluminums in the four-membered rings of the UT-6 framework that share two bridging fluorine atoms. The resulting negative charge on the framework is balanced by pyridinium cations that reside in the chabazite cages. Upon thermal treatment of UT-6, pyridine molecules and HF are removed from the structure and the material transforms into rhombohedral $\text{AlPO}_4\text{-CHA}$, as evidenced by *in situ* high-temperature powder X-ray diffraction, thermogravimetry and mass spectrometry. This represents the first solid-state transformation of an anionic aluminophosphate molecular sieve framework to an entirely neutral one.

The synthetic open-framework aluminophosphates have traditionally been prepared by aqueous methods.^{1,2} Only in recent years have non-aqueous synthetic systems been used to isolate these materials, and a series of new structures have been reported.^{3–9} Many of these crystal structures are two-dimensional layered aluminophosphates,^{5–9} and there are only two examples of a polymeric chain structure.¹⁰ Similarly, non-aqueous work in our laboratory has produced a number of layered aluminophosphate structures,^{11–14} as well as the third example of a one-dimensional chain aluminophosphate.^{12,14}

Another strategy that has been successful for the preparation of novel structures is the use of fluoride ions in the reaction mixture to produce fluoroaluminophosphates. The stronger aluminium-complexing action of fluorine over that of oxygen is well known,¹⁵ making it likely that the bridging and/or terminal oxygens of aluminophosphates can be partially or fully replaced by fluorine atoms. Indeed, a series of such compounds have been reported by Guth and co-workers^{16,17} and by others.^{8,18–22} Most of these materials are frameworks, while more recent examples correspond to layered fluoroaluminophosphates, as reported by Férey and co-workers.^{19,21} In these structures, the fluorine atoms typically occupy one¹⁸ or two^{19,21,22} vertices of the aluminium octahedra. Interestingly, aluminium tetrahedra with one oxygen atom replaced by a terminal fluorine are also present in one of the layer structures.²¹

The aqueous synthesis of a triclinic aluminophosphate with the chabazite-like topology in the presence of HF and with morpholine as a template was reported by Kessler.²³ Based on the Reitveld refinement data, it was proposed that in this novel structure, two fluorine atoms bridge two aluminums of a four T-atom ring (T=Al, P) that connects two double six-rings of the chabazite structure. This was confirmed later by ^{27}Al MAS NMR spectroscopy.^{17,24,25} The crystal structure of the material was not reported in the literature and, presumably, has yet to be precisely solved.

In the course of our non-aqueous synthetic work, we have isolated a fluorinated aluminophosphate material whose structure is closely related to $\text{AlPO}_4\text{-CHA}$. The material may be

isolated from several solvent systems, including tetraethylene glycol (TEG) and pyridine. The synthesis involves the use of a pyridine–hydrogen fluoride organic additive,¹¹ resulting in the formation of phase-pure UT-6. Large crystals, up to 400 µm, were obtained which were of sufficient size to solve the structure by single-crystal X-ray diffraction (SCXRD). It was also found that upon thermal treatment, UT-6 undergoes dehydrofluorination making the material potentially useful as a solid source of hydrogen fluoride.

Experimental

Synthesis of UT-6 from TEG solvent

All synthetic reagents were used as received. The ideal synthesis mixture for this system was $14\text{HO}(\text{CH}_2\text{CH}_2\text{O})_4\text{H}$ (TEG): $0.9\text{Al}_2\text{O}_3 \cdot 2.5\text{H}_2\text{O}$: $1.8\text{P}_2\text{O}_5$: $8.0\text{C}_5\text{H}_5\text{N}$: 1.0HF-Py . Hydrogen fluoride was added under a nitrogen atmosphere to the TEG solvent (99% purity, Aldrich or Sigma) in the form of hydrogen fluoride–pyridine (70:30 mass% HF–Py, Aldrich). The alumina source ($\text{Al}_2\text{O}_3 \cdot 2.5\text{H}_2\text{O}$, Dispal 23N4–80, Vista) was then slurried into the TEG solvent, with magnetic stirring. Phosphoric acid (85 mass% H_3PO_4 –15 mass% H_2O , Aldrich) was added dropwise, and the mixture was stirred manually to homogeneity. Finally, pyridine (BDH assured) was added, transforming the mixture into a viscous, opaque, pale yellow gel. The amount of pyridine already added from the HF–Py source was not subtracted from the 8.0 moles of pyridine, but gave similar results if it was taken into account. The homogenized gels were loaded into 15 ml capacity PTFE-lined stainless steel autoclaves, and treated under static conditions at 180 °C for 2–6 days. The powdery, pale yellow product was recovered by filtration, washing with water and acetone and was dried under ambient conditions. Individual crystals appeared to be colourless in the optical microscope, and the pale yellow colour was therefore attributed to the bulk product.

Synthesis of UT-6 from pyridine solvent

The reagents used in this system were the same as above. The synthesis mixture which yielded the highest quality

UT-6 material when pyridine was used as the solvent was $16 \text{ C}_5\text{H}_5\text{N} : 0.5\text{Al}_2\text{O}_3 : 2.5\text{H}_2\text{O} : 0.6\text{P}_2\text{O}_5 : 8.0\text{H}_2\text{O} : 2.0\text{HF} - \text{Py} : 0.0-4.0 \text{ R}$ [$\text{R} = \text{Et}_3\text{N}$ (triethylamine, 99%, Aldrich) or $\text{C}_6\text{H}_{11}\text{NH}_2$ (cyclohexylamine, 99 + %, Aldrich)]. The synthesis procedure was nearly identical to that outlined above, except the TEG was replaced with pyridine as the starting solvent. Additionally, reagent amounts of deionized water were mixed dropwise, with stirring, after addition of the hydrogen fluoride-pyridine, and the second organic additive was incorporated in the final step. Ideal synthesis conditions were 4–6 days, 150°C in the case of triethylamine, and 4–6 days, 180°C in the case of cyclohexylamine.

Characterization of UT-6

Powder X-ray diffraction (PXRD) patterns were collected on a Siemens D5000 diffractometer (Cu-K α radiation, $\lambda = 1.54178 \text{ \AA}$). The step size used was 0.030° , step time 1.0 s and scan range $1-50^\circ (2\theta)$. The detector in the instrument was a Kevex 2005-212 solid-state detector. High-temperature (HT-) PXRD patterns were obtained by running samples *in situ* on the same instrument under a nitrogen flow, using a Siemens HTK 10 attachment. The heating rate typically used was $10^\circ\text{C min}^{-1}$ between scans, and 1°C min^{-1} during data collection. Quick scans were run from 1 to $37^\circ (2\theta)$, with a 0.050° step size and a 0.7 s step time. The upper operating limit of the HTK 10 attachment was 1200°C .

Thermogravimetry (TG) was performed on a Perkin-Elmer 7 Series analyser, under a nitrogen atmosphere and with a 5°C min^{-1} heating rate.

Scanning electron microscopy (SEM) and energy-dispersive X-ray analysis (EDXA) were performed on a JEOL 840 scanning electron microscope, with accelerating conditions of 10^{-10} A and 5 kV.

SCXRD data were collected on an Enraf-Nonius CAD4 diffractometer using graphite-monochromated Mo-K α radiation ($\lambda = 0.71073 \text{ \AA}$). A summary of selected crystallographic data is given in Table 1. The intensities of three standard reflections measured every 120 min showed no decay. The data were corrected for Lorentz and polarization effects and a semi-empirical absorption correction was applied.

The structure was solved using the SHELXTL/PC V5.0 package²⁶ and refined by full-matrix least squares on F^2 using all data (negative intensities included). The weighting scheme was $w = 1/[\sigma^2(F_o^2) + (aP)^2 + bP]$ where $P = (F_o^2 + 2F_c^2)/3$. Hydrogen atoms were included in calculated positions and treated as riding atoms. The hydrogen atoms from the partial occupancy water molecule were not included in the refinement but were included in the molecular formula.

Results and Discussion

The synthesis conditions given above for both the TEG and pyridine solvent systems are ideal for obtaining the UT-6 material in high yields and, on average, below $50 \mu\text{m}$ in size [PXRD patterns, Fig. 1(a), (b), respectively and SEM, Fig. 2(a)]. For the TEG product, a trace amount of the layered pyridinium aluminophosphate of Chippindale *et al.*⁶ exists in the product, for which only the 100% peak appears, comparing Fig. 1(a) and (d) (see below). Interestingly, products obtained from pyridine solvent are phase-pure [Fig. 1(b)], and are of higher crystallinity, giving rise to a more intense diffraction pattern. The differences in relative intensities in the PXRD patterns of Fig. 1(a) and 1(b) can also be attributed to the differences in the crystal morphology leading to preferred orientation of the crystals in the samples which we were not able to avoid.

For the TEG solvent system, depending on the synthesis conditions such as temperature, water concentration and number of moles of template, the layered pyridinium aluminophosphate and/or berlinite were obtained as impurities or as major products. For the pyridine solvent system, use of more than 4.0 moles of the second organic additive (R) resulted in partial or complete change of the product to aluminophosphate phases templated by the second organic additive. For example,

Table 1 Summary of crystal data, details of intensity collection and least-squares refinement parameters of UT-6

empirical formula	$\text{C}_5\text{H}_6\text{Al}_3\text{FNO}_{12}\text{P}_3 \cdot 0.15\text{H}_2\text{O}$
M_r	467.66
crystal size/mm	$0.40 \times 0.10 \times 0.10$
crystal class	triclinic
space group	$P\bar{1}$
T/K	293(2)
$a/\text{\AA}$	9.118(1)
$b/\text{\AA}$	9.161(1)
$c/\text{\AA}$	9.335(1)
$\alpha/\text{degrees}$	85.98(1)
$\beta/\text{degrees}$	77.45(1)
$\gamma/\text{degrees}$	89.01(1)
$V/\text{\AA}^3$	759.25(14)
Z	2
$D_c/\text{g cm}^{-3}$	2.046
$\mu(\text{Mo-K}\alpha)/\text{cm}^{-1}$	6.44
$F(000)$	467
ω scan width/degrees	$0.59 + 0.50\tan\theta$
range θ collected/degrees	2.23–26.30
absorption correction	psi scans
min., max. transmission	0.596, 0.616
no. reflections collected	3292
independent reflections	3087
R_{int}	0.0159
no. observed data [$I > 2\sigma(I)$]	2725
R_1 [$I > 2\sigma(I)$] ^a	0.0280
wR_2 (all data) ^a	0.0830
weighting a, b	0.0372, 0.92
goodness of fit	1.072
parameters refined	232
max. density in ΔF map/ $e \text{ \AA}^{-3}$	0.454

^aDefinition of R indices: $R_1 = \Sigma(F_o - F_c)/\Sigma(F_o)$, $wR_2 = \{\Sigma[w(F_o^2 - F_c^2)^2]/\Sigma[w(F_o^2)^2]\}^{1/2}$.

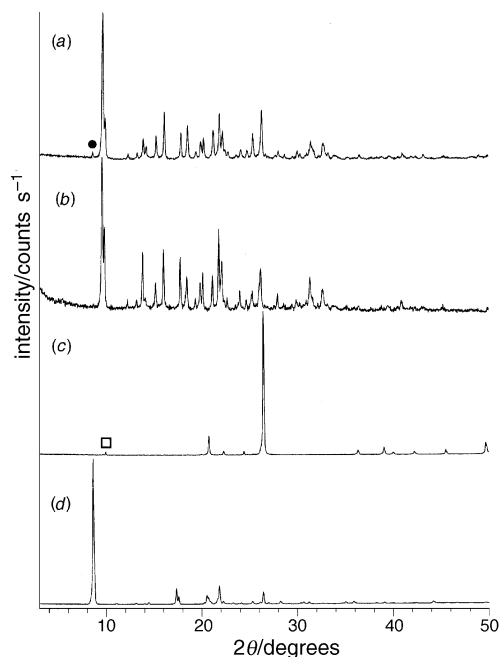


Fig. 1 PXRD patterns of representative synthesis products: (a) UT-6 isolated from the TEG system when 1.0 HF is used; a small amount of the layered pyridinium aluminophosphate⁶ is also obtained (●); (b) UT-6 isolated from the pyridine solvent system, showing excellent crystallinity and no impurities; (c) no HF added, which yields a majority phase of berlinite, and trace 'impurity' amounts of UT-6 (□); (d) the product using a new PTFE liner, containing no UT-6 fluoroaluminophosphate, and only the layered pyridinium aluminophosphate material⁶

phosphate and/or berlinite were obtained as impurities or as major products. For the pyridine solvent system, use of more than 4.0 moles of the second organic additive (R) resulted in partial or complete change of the product to aluminophosphate phases templated by the second organic additive. For example,

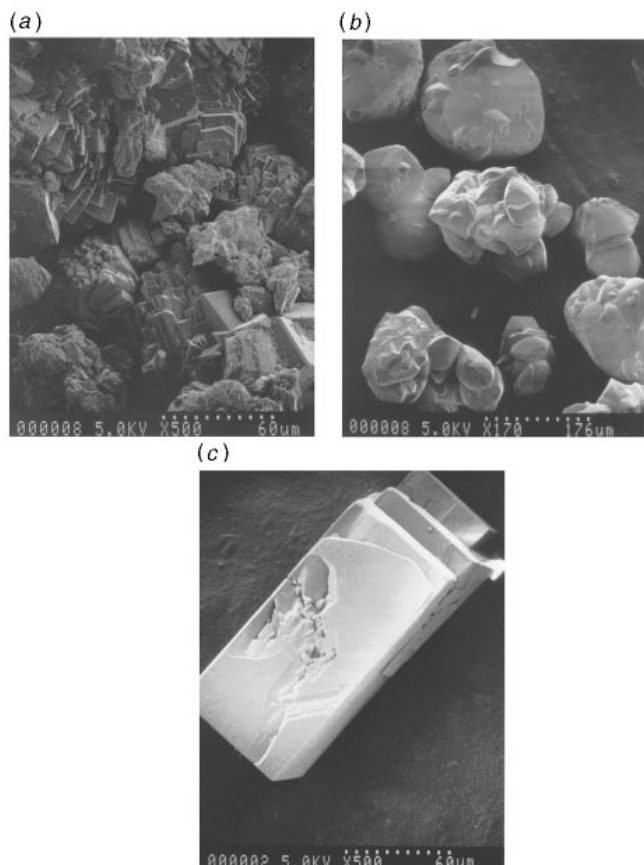


Fig. 2 Scanning electron micrographs: (a) UT-6 crystals obtained from the TEG-1.0 HF system; (b) berlinite crystals obtained as majority phase when no HF was added; (c) large UT-6 crystals which allowed SCXRD data collection, obtained in trace amounts when no HF was added

in the presence of cyclohexylamine, the layered aluminophosphates UT-4 and UT-5, which we have recently isolated from the TEG-cyclohexylamine synthesis system,¹³ were the dominant phases. Similar effects were observed by varying temperatures when 4.0 moles of organic additive were used. In the case of triethylamine, increasing the temperature above the ideal 150 °C led to triethylamine-related aluminophosphate phases, while in the case of cyclohexylamine, decreasing the temperature from the ideal 180 °C led to cyclohexylamine-related phases.

To obtain crystals large enough for SCXRD study, it was necessary to change the synthesis conditions as follows. UT-6 was initially isolated from the TEG-pyridine reaction mixture without HF being added to it (molar composition: 14 TEG : 0.9Al₂O₃ : 2.5H₂O : 1.8P₂O₅ : 8.0C₅H₅N). In this initial experiment, the majority product was berlinite [PXRD, Fig. 1(c)]. The particles were large, faceted crystals typically obtained for this dense phase [SEM, Fig. 2(b)]. However, a limited number of ca. 200–400 μm plate-like fluoroaluminophosphate UT-6 crystals [SEM, Fig. 2(c)] coprecipitated with the berlinite, as can be seen in the PXRD pattern [Fig. 1(c)]. These large crystals were manually separated from the product, allowing study by SCXRD.

The formation of UT-6 despite the fact that no source of fluorine was added to the liner, might be due to the presence of impurities in the walls of the PTFE liner. These impurities could be introduced by the reaction mixtures of prior synthetic runs used for the particular liner. In accord with this, the use of a new and unused PTFE liner yielded only the layered pyridinium-aluminophosphate,⁶ and no fluorinated UT-6 [Fig. 1(d)]. We have also found that the deliberate contami-

nation of the PTFE liner with HF prior to its use has a marked influence on the structures that are obtained in this and other aluminophosphate systems.²⁷ Work is currently under way to quantify the exact amounts of HF-Py necessary to use in order to obtain a berlinite majority phase with a trace amount of large UT-6 crystals. However, it should also be noted that there may be a slow release of fluorine occurring in the process, and work is also under way in this respect.

The large crystal size and concomitant strong diffraction allowed for a full structure refinement with a low *R*-factor. Positions of the hydrogen atoms of the protonated pyridinium and of the unexpected bridging fluorine atoms (as opposed to similarly diffracting oxygen) were determined by using a difference Fourier map technique. The ¹⁹F MAS NMR data provided supporting evidence for the presence of the F atoms in the interstices of the framework. The ¹⁹F MAS NMR spectrum of UT-6 is shown in Fig. 3. It contains one strong peak at ca. –120 ppm, referenced to C₆F₆, and is in good agreement with the data of Klock *et al.*²⁸ The presence of fluorine is also reflected in the elemental analysis of the as-synthesized UT-6 material (F: 1.53%; C: 13.56%; N: 2.51%).

The thermal ellipsoids and views of the structure are shown in Plate 1. The framework contains three independent eight-membered ring channel systems. The empirical formula [Al₃P₃O₁₂F][–] reflects the negative charge of the framework, which is charge-balanced by the pyridinium cations. Two template molecules are observed to reside in each cage, pointing to opposite corners [Plate 1(c)], as related by the inversion centre of the *P* $\bar{1}$ space group. Atomic coordinates, thermal parameters, and bond lengths and angles have been deposited at the Cambridge Crystallographic Data Centre (CCDC). See Information for Authors, *J. Mater. Chem.*, 1997, Issue 1. Any request to the CCDC for this material should quote the full literature citation and the reference number 11451/28. The experimental PXRD pattern of UT-6 may be fully indexed to the computer-simulated pattern based on the SCXRD structure.

The structure of the UT-6 framework is related to the neutral aluminophosphate analogue of the microporous zeolite chabazite, which we denote AlPO₄-CHA, since it exists in several forms such as AlPO₄-34 or the metal-substituted MAPO-34, MAPO-44 or MAPO-47 structure types.²⁹ The AlPO₄-CHA framework contains alternating tetrahedral Al and P atoms connected by bridging oxygens to define an array of hexagonal prisms connected by four-rings. In UT-6, however, each six-ring of the hexagonal prisms contains one octahedral aluminium that connects to that of another hexagonal prism, through two bridging fluorines [Al–F 1.854(2), 1.894(2) Å] [Plate 1(b)]. The octahedra are thereby dimerized into double octahedra, while the remaining aluminium atoms are tetra-

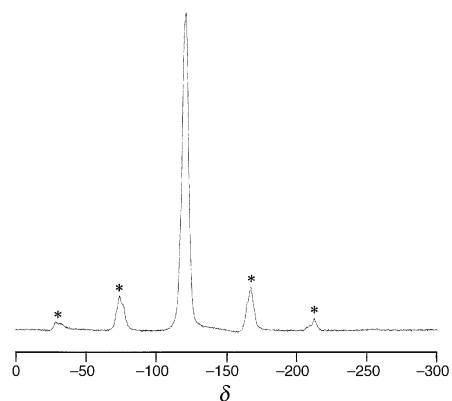


Fig. 3 ¹⁹F MAS NMR spectrum of as-synthesized UT-6 obtained from the TEG system. Spectrum collected at 376.4 MHz, with 17 kHz spinning rate, 3.0 μs pulse duration and 4.0 s recycle time and referenced to C₆F₆. Asterisks denote spinning sidebands.

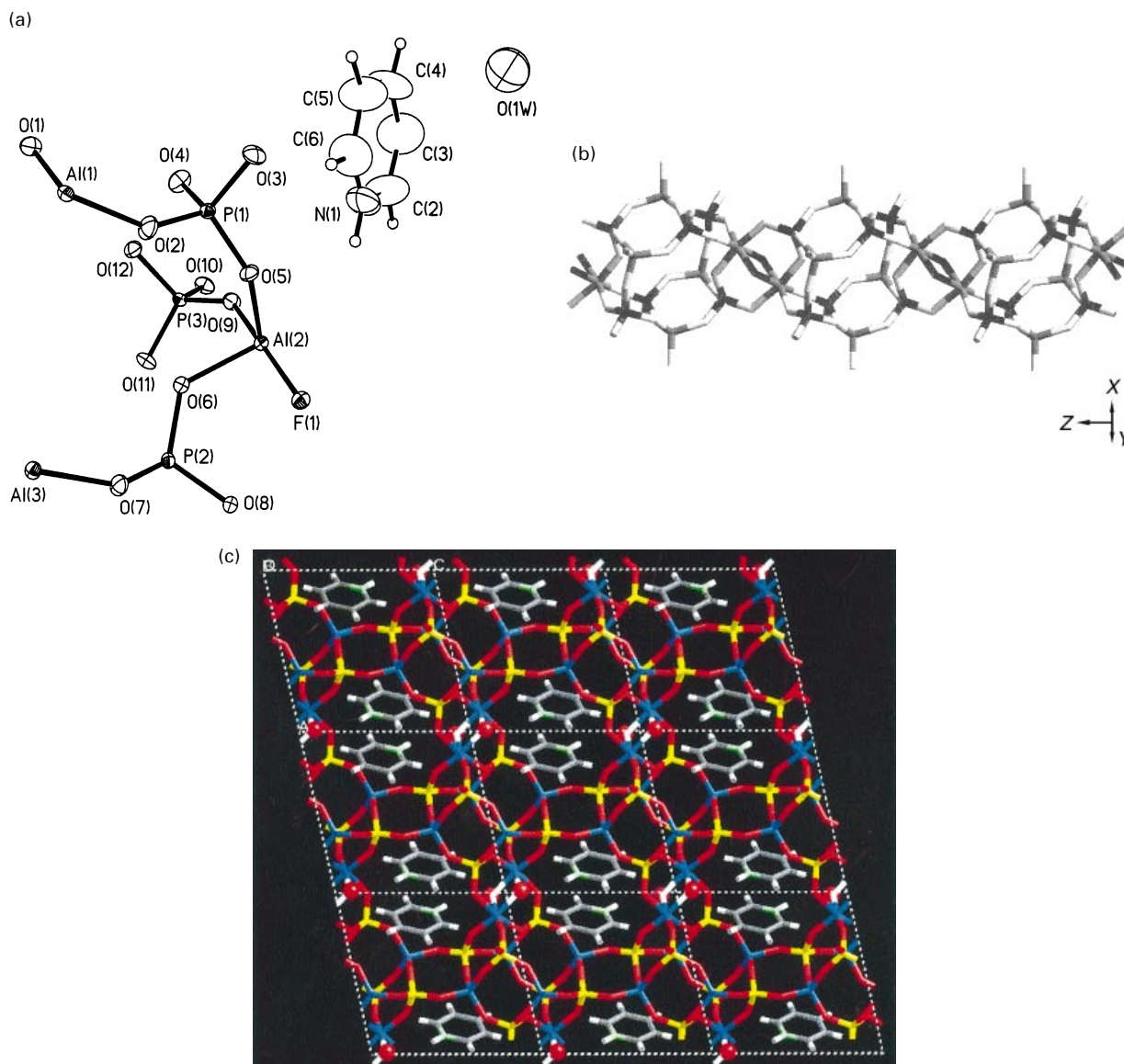


Plate 1 (a) Thermal ellipsoids and labelling of the asymmetric unit; (b) a view of two hexagonal prisms, and the nature of their connection through Al-(μ -F)-Al links. Shading scheme: oxygen, white; fluorine, black; aluminium, grey; phosphorus, black; (c) CERIOUS [010] crystallographic projection of the UT-6 structure. The isolated spheres represent oxygens of intrachannel water molecules that were resolved in the structure refinement. Colour scheme: oxygen, red; phosphorus, yellow; aluminium, blue; fluorine, white; nitrogen, green; hydrogen, white; carbon, grey.

hedrally coordinated by four oxygens. As observed in $\text{AlPO}_4\text{-CHA}$, the hexagonal prisms are tilted and define a three-dimensional framework. The three channel systems intersect to form chabazite-like cages in which the templates reside. The electrostatically bonded pyridiniums are also strongly hydrogen bonded to a bridging oxygen of the octahedral aluminiums, one for each aluminium ($\text{N-H}\cdots\text{O}_{\text{av}}$ 1.849 Å).

The solid-state NMR spectrum of the UT-6 material obtained from TEG showed one peak for each crystallographically unique metal atom, as expected. The ^{31}P CP MAS NMR spectrum showed three strong and sharp resonances of equal intensity at *ca.* -8.5, -25.2 and -31.1 ppm (referenced to $[\text{NH}_4][\text{H}_2\text{PO}_4]$, 400.13 MHz, 10 kHz spinning rate, 3.0 μs pulse duration and 4.0 s recycle time), and were typical for aluminophosphate materials.³⁰ The fluorine-decoupled ^{27}Al MAS NMR spectrum showed two peaks at *ca.* 29.5 and -17.9 ppm (referenced to Al_2O_3 , 17 kHz spinning rate), in an approximately 2:1 intensity ratio. The former downfield peak was resolved into two peaks by a ^{27}Al MQ MAS experiment. The values also agree with published values,³⁰ where the two peaks resolved by MQ MAS are due to the two crystallographically

unique tetrahedral aluminiums, and the upfield peak is due to the one type of octahedral aluminium.

Since the framework is anionic, it is intuitive that the cations may be ion-exchanged. Although charged aluminophosphate frameworks are known to exist,^{8,22,31,32} ion exchange of these materials is unlikely or not possible owing to the restricted dimensions of the eight-membered ring channels, which reduces the free aperture for the diffusion of molecules through the structure. The relative openness of UT-6, however, may render the material potentially applicable, for example as an ion-exchanger. Further work is under way in this regard.

Owing to the microporous nature of the material, it is possible to remove the organic template molecules by calcination. The van der Waals size of the planar pyridinium cations (*ca.* 6.3 Å in the largest dimension) is smaller than the free aperture of the eight-ring windows between the chabazite-like cages (*ca.* 6.5–6.9 Å). However, the negative charge of the framework would have to be compensated or removed in the process. The TG curve of the material (Fig. 4) shows that a thermal event occurs just above 400 °C, which may be attributed to loss of the extra-framework pyridiniums and

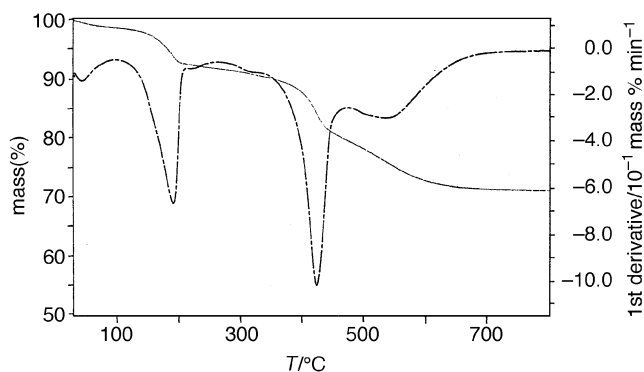


Fig. 4 TG trace of UT-6, displaying thermal events at ca. 150°C and 400°C

framework fluorines (observed mass loss: 20.3 mass%; expected: 20.5 mass%). This event in the *in situ* HTPXRD pattern corresponds to a phase transformation from UT-6 to a fully indexable $\text{AlPO}_4\text{-CHA}$ (Fig. 5). Mass spectrometry of the product from TEG confirms the release of pyridine and hydrogen fluoride at these temperatures. The loss of both would have to occur in order to transform UT-6 to the entirely oxide-based $\text{AlPO}_4\text{-CHA}$ framework. The TG event at approximately 150°C with the loss of ca. 6 mass% presumably corresponds to loss of the intra-channel H_2O that was observed in the SCXRD refinement. The HTPXRD pattern remains unchanged through this event (Fig. 5), so the UT-6 structure must be maintained, and the unit cell unchanged.

This dehydrofluorination is unique on two counts: first, as a solid source of hydrogen fluoride, and secondly, as the first solid-state transformation of an anionic molecular sieve framework to an entirely neutral molecular sieve. Interestingly, the resulting $\text{AlPO}_4\text{-CHA}$ structure is observed to be intact still at 1200°C (Fig. 5).

Conclusions

The structure of a novel fluoroaluminophosphate UT-6 molecular sieve has been solved by SCXRD methods. The material is readily prepared from several non-aqueous solvents systems, including pyridine and TEG. High-temperature studies of the material show a unique dehydrofluorination process to occur,

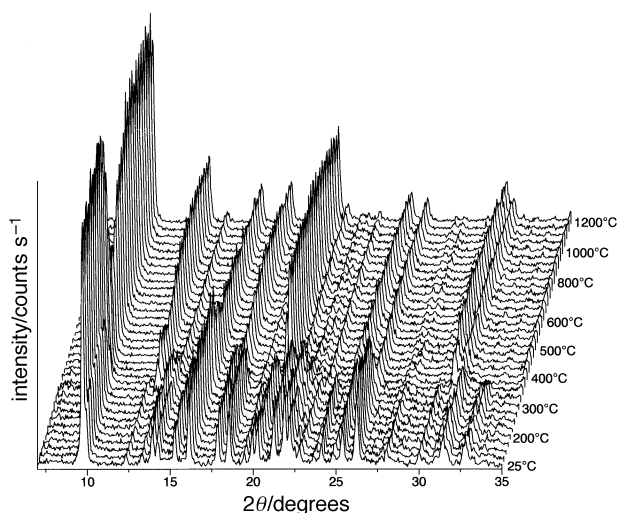


Fig. 5 *In situ* high-temperature PXRD of UT-6. The material cleanly and completely transforms to $\text{AlPO}_4\text{-CHA}$ in the 400°C region, indicative of the UT-6 dehydrofluorination process. The $\text{AlPO}_4\text{-CHA}$ structure is still intact at 1200°C.

where the anionic framework is transformed to the neutral oxide CHA-type aluminophosphate framework. This may render the framework useful as a solid source of hydrogen fluoride. Similar results were reported in the literature for the morpholine-containing material synthesized in an aqueous reaction medium, so the structural details reported in this paper should also be relevant to the structure of that material.

Financial assistance from the Natural Sciences and Engineering Research Council of Canada in support of this work is acknowledged. S.O. expresses his appreciation to the Ontario Graduate Scholarship program in partial support of his research. We thank Dr. Neil Coombs (Imagetek Analytical Imaging, Toronto) for scanning electron microscopy, Bruker Instruments, Inc. for solid-state NMR data and Dr. David Young for informative discussions.

References

- 1 S. T. Wilson, B. M. Lok, C. A. Messina, T. R. Cannan and E. M. Flanigen, *J. Am. Chem. Soc.*, 1982, **104**, 1146.
- 2 S. T. Wilson, B. Lok and E. M. Flanigen, *US Pat.*, 1982, 4 310 440.
- 3 R. H. Jones, J. M. Thomas, J. Chen, R. Xu, Q. Huo, S. Li, Z. Ma and A. M. Chippindale, *J. Solid State Chem.*, 1993, **102**, 204.
- 4 A. M. Chippindale, A. V. Powell, R. H. Jones, J. M. Thomas, A. K. Cheetham, Q. Huo and R. Xu, *Acta Crystallogr., Sect. C: Cryst. Struct. Commun.*, 1994, **50**, 1537.
- 5 R. H. Jones, J. M. Thomas, R. Xu, Q. Huo, A. K. Cheetham and A. V. Powell, *J. Chem. Soc., Chem. Commun.*, 1991, 1266.
- 6 A. M. Chippindale, A. V. Powell, L. M. Bull, R. H. Jones, A. K. Cheetham, J. M. Thomas and R. Xu, *J. Solid State Chem.*, 1992, **96**, 199.
- 7 A. M. Chippindale, S. Natarajan, J. M. Thomas and R. H. Jones, *J. Solid State Chem.*, 1994, **111**, 18.
- 8 J. Paillaud, B. Marler and H. Kessler, *Chem. Commun.*, 1996, 1293.
- 9 I. D. Williams, Q. Gao, J. Chen, L. Ngai, Z. Lin and R. Xu, *Chem. Commun.*, 1996, 1781.
- 10 R. H. Jones, J. M. Thomas, R. Xu, Q. Huo, Y. Xu, A. K. Cheetham and D. Bieber, *J. Chem. Soc., Chem. Commun.*, 1990, 1170.
- 11 A. Kuperman, S. Nadimi, S. Oliver, G. A. Ozin, J. M. Garces and M. M. Olken, *Nature (London)*, 1993, **365**, 239.
- 12 (a) S. Oliver, A. Kuperman, A. Lough and G. A. Ozin, *Chem. Mater.*, 1996, **8**, 2391; (b) R. Kniep and M. Steffen, *Angew. Chem., Int. Ed. Engl.*, 1978, **17**, 272.
- 13 S. Oliver, A. Kuperman, A. Lough and G. A. Ozin, *Chem. Commun.*, 1996, 1761.
- 14 S. Oliver, A. Kuperman, A. Lough and G. A. Ozin, *Inorg. Chem.*, 1996, **35**, 6373.
- 15 N. N. Greenwood and A. Earnshaw, *Chemistry of the Elements*, Pergamon Press, New York, 1984, p. 938.
- 16 S. Qiu, W. Pang, H. Kessler and J. L. Guth, *Zeolites*, 1989, **9**, 440.
- 17 J. L. Guth, H. Kessler, P. Caullet, J. Hazm, A. Merrouche and J. Patarin, in *Proceedings of the 9th International Zeolite Conference*, ed. R. von Ballmoos, J. B. Higgins and M. M. J. Treacy, Butterworth-Heinemann, London, 1993, vol. I, p. 215.
- 18 L. Yu, W. Pang and L. Li, *J. Solid State Chem.*, 1990, **87**, 241.
- 19 D. Riou, Th. Loiseau and G. Ferey, *J. Solid State Chem.*, 1993, **102**, 4.
- 20 G. Ferey, *J. Fluorine Chem.*, 1995, **72**, 187.
- 21 J. Renaudin and G. Ferey, *J. Solid State Chem.*, 1995, **120**, 197.
- 22 S. J. Kirkby, A. J. Lough and G. A. Ozin, *Z. Kristallogr.*, 1995, **210**, 956.
- 23 H. Kessler, in *Synthesis/Characterization and Novel Applications of Molecular Sieves*, ed. R. L. Bedard, T. Bein, M. E. Davis, J. Garces, V. A. Maroni and G. D. Stucky, *Mater. Res. Soc. Symp. Proc.*, Materials Research Society, Pittsburgh, PA, 1991, **233**, 47.
- 24 L. Delmotte, M. Souillard, F. Guth, A. Seive, A. Lopez and J. L. Guth, *Zeolites*, 1990, **10**, 778.
- 25 C. Fernandez, J. P. Amoureux, L. Delmotte and H. Kessler, *Microporous Mater.*, 1996, **6**, 125.
- 26 Sheldrick, G. M. SHELXTL/PC Version 5.0, Siemens Analytical X-Ray Instruments Inc., Madison, WI, 1995.
- 27 S. Oliver, PhD Thesis, University of Toronto, 1997.
- 28 E. Klock, L. Delmotte, M. Souillard and J. L. Guth, in *Proceedings*

- of the 9th International Zeolite Conference, ed. R. von Ballmoos, J. B. Higgins and M. M. J. Treacy, Butterworth-Heinemann, London, 1993, vol. 1, p.611.
- 29 R. Szostak, *Handbook of Molecular Sieves*, Van Nostrand Reinhold, New York, 1992.
- 30 C. S. Blackwell and R. L. Patton, *J. Phys. Chem.*, 1988, **92**, 3965, and references therein.
- 31 J. B. Parise, *Acta Crystallogr. Sect. C: Cryst. Struct. Commun.*, 1984, **40**, 1641.
- 32 S. Natarajan, J. P. Gabriel and A. K. Cheetham, *Chem. Commun.*, 1996, 1415.

Paper 6/06828F; Received 7th October, 1996